Scientific Research Publishing

International Journal of Astronomy and Astrophysics, 2019, 9, 247-264
http://www.scirp.org/journal/ijaa
ISSN Online: 2161-4725
ISSN Print: 2161-4717

Gamma-Ray Bursts Generated by Hyper-Accreting Kerr Black Hole

Feyiso Sado

Department of Physics, Addis Ababa University, Addis Ababa, Ethiopia
Email: bsfeyiso@gmail.com

How to cite this paper: Sado, F. (2019) Gamma-Ray Bursts Generated by Hyper-Accreting Kerr Black Hole. *International Journal of Astronomy and Astrophysics*, **9**, 247-264.
https://doi.org/10.4236/ijaa.2019.93018

Received: April 27, 2019
Accepted: September 2, 2019
Published: September 5, 2019

Abstract

The observed properties of Gamma-Ray Bursts such as rapid variability of X-ray light curve and large energies strongly signature the compact binary, disk accreting system. Our work particularly highlights the extremely rotating, disk accreting black holes as physical source of the flares variability and X-ray afterglow plateaus of GRBs. We investigate the compact binary mergers (neutron star - neutron star and neutron star onto black hole) and gravitational core collapse of super massive star, where in both cases hyper-accreting Kerr hole is formed. The core collapse in a powerful gravitational wave explained as a potential source for the radiated flux of hard X-rays spectrum. We described the evolution of rapidly rotating, accreting BH in general relativity and the relativistic accretion flow in resistive MHD for viscous radiation. We compute the structure of accretion disk, the accretion luminosity of the dynamical evolution of inner accretion disk and precisely determine their radiation spectra, and compare to observational data of X-ray satellites. Finally, we obtained the resulting disk radiation basically explained as the X-ray luminosity of the central source, such as LMC X-1 and GRO J1655-40. These results are interestingly consistent with observational data of galactic X-ray source binary systems such as X-ray luminosities of Cygnus X-1 and Seyfert galaxies (NGC 3783, NGC 4151, NGC 4486 (Messier 87)) which are powerful emitters in X-ray and gamma-ray wavebands of the observed X-ray variability with typical luminosity.

Keywords

Relativistic Disk Accreting BH-Gamma Rays, Bursts-Radiation, X-Ray Luminosity

1. Introduction

Different theories for the gamma-ray bursts (GRBs) progenitor systems emerged

using the observational results, with the leading models involving a compact object merger for the short bursts [1] [2] [3] [4] and a massive star core collapse (collapsar model) [5] [6] to a compact object (black hole or neutron star) origin for the long bursts. A new intimation into the progenitors that emit GRBs came from the compact stellar and host galaxy coincidence of GRB 980425 with the supernova SN 1998 bw [7] that resembles the ordinary Type Ic SN 1994I or the weak version of hypernova, SN 2002ap [8] and recently observed gravitational wave [9].

Beside collapsar and merger progenitor types, the accretion-induced collapse of a rapidly rotating white dwarf and neutron star scenarios is also extensively studied [10]. Long duration GRBs associated with type Ib/c supernovae (SNe) are powered by collapsars [11]. The compact binary mergers are the promising sources of short GRBs [12] [13]. Therefore, main classes of possible progenitors models have been proposed for the origin of gamma-ray bursts are two neutron stars or neutron star-black hole mergers and massive star gravitational core collapse (hypernova). These prospective progenitor system activities capable of producing GRBs involving accretion of a massive ($\sim 0.1 M_{\odot}$) disk onto a newborn black hole can result from the explosion of a massive star core collapse, or following the coalescence of binary compact stellar remnants. In both cases a spinning black hole is formed with torus system, either from the super massive stellar core collapse or from a tidally disrupted neutron star, form a temporary accretion disk or torus which ultimately fall into the black hole, generating a fraction of its gravitational energy that power GRB AGN.

The observed X-ray light curves (Swift-XRT) of GRBs widely compact the sources producing them [14] [15] [16]. For instance the plateau and the overlying x-ray flare(s) acceptably powered by compact progenitors, identified as gravitational core collapse of a rapidly rotating super massive star [16] [17] or merged core of compact objects such as double NS, NS-BH or WD-BH [18] [19]. Based on several observational results the central binary sources of energetic burst emission was identified as gravitational core collapse of super massive star or merged core of 2NSs or NS-BH [20] as engines for short gamma-ray bursts, which are very efficient at converting high photon energy into luminous radiation. The intrinsic glowing flow of gamma rays emission from rotating, strongly magnetized disk accreting BH formed in dying super-giant stars or compact mergers [21] [22] typical disclosed, where collapsar or merger explained as prime candidates that form disk accreting black hole in AGN. The entire scenarios basically explained as the observed AGN radiation spectrum. Thus, Gamma-Ray Bursts are primal result of accretion onto black holes.

Our subject of study, a viscous, strongly magnetized disk accreting black hole discussed in [23] and it was shown that the accretion disk largely characterized by a strong magnetic field, differential rotation and shear-induced turbulent stresses. The accretion torus dynamics is potentially driven by shear stress or convection that results in luminous radiation where angular momentum transport ensures the turbulent disk formation. Previous work has shown that lu-

minous radiation of AGN and X-ray binaries are consistent with magnetized disk shear instability. Moreover, the spectrum of Cyg X-1 [24] associated with Galactic X-ray sources and large luminosity of AGN can be explained by torus disk accretion process [25]. It is also argued that X-ray flares are produced by magnetar [26] [27]. Magnetar engine deeply explored in [28] and the resulting spin-down luminosity compared with that of X-ray emission to shade light on light-curve features. These observed X-ray variability with thermal hard X-ray spectrum component has generally been interpreted as thermal emission from turbulent accretion disk [29]. But the physical sources of luminous burst radiation have not yet been well settled. Thus, we are intended to study the evolution of rapidly rotating, accreting BH in full general relativity and the relativistic accretion flow in MHD and its numerical calculation with accurate GRMHD code [30]. We approach the outflow radiation using MHD conserved equations to construct spectrum of radiative heating due to viscous and magnetic dissipation in general relativistic Kerr geometry. We compute the structure of accretion disk, the accretion luminosity of the dynamical evolution of inner accretion disk and precisely determine their radiation spectra.

The aim of this paper is to explore relativistic disk accreting Kerr black hole as the potential central source of gamma ray bursts. We begin with the detailed discussions of merger of compact binaries involving neutron stars and super massive star gravitational core collapse. Particularly, investigating super massive star gravitational core collapse leads to newly formed rapidly spinning, black holes and compact core mergers (perhaps NS-NS and NS-BH). Finally, we infer the radiative heating flux density due to viscous and magnetic energy dissipation in general relativistic Kerr Black Hole. In Section 2 we present a brief description of general relativistic resistive MHD formulations. The relativistic accretion flow in resistive MHD and the resulting radiation basically explained as the X-ray luminosity of the central source explored in Section 3. Finally, in Section 4 we provide a summary and draw the concluding remarks.

2. Relativistic MHD Disk Model

Luminous disk accretion onto rotating black holes general governed by magnetohydrodynamic (MHD) equations. This spinning, magnetized black hole with thin asymmetric turbulent relativistic disk widely simulated and MHD equations are numerically solved [25] [30]. Then, traditionally the equations of relativistic MHD are given in the conserved form: the mass continuity equation

$$\nabla_{\mu}\left(\rho u^{\mu}\right)=\sigma, \tag{1}$$

where ρ is rest mass density, u^{μ} is the 4-velocity of the fluid and σ is source or sink. The energy-momentum conservation

$$\nabla_{\mu}T^{\mu\nu}=0, \tag{2}$$

where, $\nu=0,1,2,3$, then stress-energy tensor is

$$T^{\mu\nu}=\left(\rho+\rho\varepsilon+P+b^{2}\right)u^{\mu}u^{\nu}. \tag{3}$$

The Einstein tensor $G_{\mu\nu}$ and $T_{\mu\nu}$ the total stress-energy tensor are related as

$$G_{\mu\nu} = 8\pi T_{\mu\nu}, \tag{4}$$

and the Ricci tensor

$$T_{\mu\nu} = -R_{\mu\nu} = G^{\nu}. \tag{5}$$

The Maxwell's equations calculated from Faraday tensor $F^{\mu\nu}$ follows

$$\nabla_{\mu} F^{\mu\nu} = 0, \tag{6}$$

$$\nabla_{\mu} F^{\mu\nu} = J^{\mu}, \tag{7}$$

using a covariant derivative of a vector ($A^{i}{}_{;k} = A^{i}{}_{,k} + \Gamma^{i}_{jk} A^{j}$) we obtain

$$g^{-1/2} \frac{\partial}{\partial x^{\mu}} \left[\left(P/c^2 + \rho \right) u^{\mu} u^{\nu} \right] + \frac{\partial P}{\partial x^{\mu}} g^{\mu\nu} + \Gamma^{\mu}_{\nu\lambda} \left(P/c^2 + \rho \right) u^{\nu} u^{\lambda} = 0, \tag{8}$$

is the four-vectorial mass flux-density conservation equations of relativistic fluid including gravity. Taking the dominant part of the radial component we can retrieve

$$u^0 u^0 \Gamma^2_{00} + 2u^0 u^1 \Gamma^2_{01} + u^1 u^1 \Gamma^2_{11} = 0,$$

for simplicity we take the equatorial plane, B_r, B_{θ}, v_r and v_{θ}.

$$\frac{\partial \rho}{\partial t} + \nabla \cdot \left(\rho \upsilon \right) = 0,$$

$$\frac{\partial \rho}{\partial t} + \frac{1}{r^2} \frac{\partial}{\partial t} \left(r^2 \rho \upsilon_r \right) = 0, \tag{9}$$

this follows from mass accretion rate $\dot{M} = -\int \rho \upsilon \cdot \mathrm{d}A$. The momentum conservation equation for magnetized plasma where matter interacts with electromagnetic field is calculated from partial time derivative of ($\gamma \rho \upsilon$) and the continuity equation

$$\gamma^2 \left(\rho + P/c^2 \right) \left[\frac{\partial \boldsymbol{v}}{\partial t} + \left(\boldsymbol{v} \cdot \nabla \right) v \right] = -\nabla \boldsymbol{P} - \rho F_g + \boldsymbol{j} \times \boldsymbol{B} + \rho \boldsymbol{E} - \frac{v}{c^2} \left(\boldsymbol{E} \cdot \boldsymbol{j} \right), \tag{10}$$

including all magnetorotation instability in resistive MHD: corotation field

$$\boldsymbol{E} \cdot \boldsymbol{J} = \eta \boldsymbol{J}^2 + B_r B_{\phi}, \tag{11}$$

the 2nd term is from magnetic tension force. Similarly, the equation of energy conservation follows from the partial time derivative of the total internal energy density (energy per unit mass) of the fluid

$$\varepsilon = \frac{1}{2} \rho \upsilon^2 + \frac{P}{\gamma - 1} + \frac{B^2}{8\pi} + \rho \Phi_g, \tag{12}$$

comprising kinetic, the internal specific enthalpy, magnetic and potential energies, respectively. Thus, the energy conservation equation is then

$$\frac{\partial \varepsilon}{\partial t} + \nabla \cdot \left(\boldsymbol{S} + P\boldsymbol{v} + \rho \Phi_g \boldsymbol{v} \right) = \nabla \cdot \left(\boldsymbol{v} \cdot \boldsymbol{t} - \boldsymbol{h} \right), \tag{13}$$

where

$$\boldsymbol{S}=\left(\frac{1}{2}\rho(\gamma\upsilon)^2+\frac{\gamma P}{\gamma-1}\right)\boldsymbol{v}+\frac{1}{\mu_0}\boldsymbol{B}\times(\boldsymbol{v}\times\boldsymbol{B}),$$

is the total energy flux and consists of the macroscopic transport of the total energy with velocity, the work done by the pressure and magnetic forces and vector $\boldsymbol{h}$ is the net thermal heat flux exchanged by the element of fluid per unit time per unit area,

$$h=\int\frac{m}{2}v'^2\boldsymbol{v}\varepsilon(t,r,v)\mathrm{d}A,$$

represents energy transport equation. The pressure is

$P=(\Gamma-1)\left(\varepsilon-\left(\frac{1}{2}\rho(\gamma\upsilon)^2-B^2/2\right)\right)$ with partial differential

$$\frac{\partial v_\alpha P_{\alpha\beta}}{\partial x_\beta}=\frac{\partial}{\partial x_\beta}\left(Pv_\beta+T_{\alpha\beta}v_\beta\right).$$

These fundamental general relativistic MHD conservation equations can be expressed as a hyperbolic, first-order, flux-conservative partial differential equation

$$\frac{\partial\boldsymbol{U}}{\partial t}+\nabla\cdot\boldsymbol{F}(U)=\boldsymbol{S}(U),\tag{14}$$

where $\boldsymbol{U}$ denotes a state vector as function of MHD conserved variables (ρ,P,υ^i,B^i) and $\boldsymbol{F}$ is the flux vector, with the five-dimensional state vector $U=\left[D,S_j,\rho E,B\right]$, which are a system of hyperbolic partial differential equations. The flux vector $\boldsymbol{F}$ is

$$\boldsymbol{F}=\begin{pmatrix}Dv^i\\ S_jv^i+P\delta^i_j-b_jB^i/\gamma\\ Ev^i+P\upsilon^i-b^0B^i/\gamma-\gamma\rho v^i\\ \upsilon^iB^k-\upsilon^kB^i\end{pmatrix},\tag{15}$$

where S_j is Poynting flux and $b^0=\gamma B^iv_k$, $b^i=B^i/\gamma+\gamma B^iv_kv^i$ are magnetic field in fluid's rest frame. The source term $\boldsymbol{S}$ is also

$$\boldsymbol{S}=\begin{pmatrix}0\\ T^{\mu\nu}\left(\frac{\partial g_{\nu j}}{\partial x^\mu}-\Gamma^\delta_{\nu\mu}g_{\delta j}\right)\\ \alpha\left(T^{\mu0}\frac{\partial\ln\alpha}{\partial x^\mu}-T^{\mu\nu}\Gamma^0_{\nu\mu}\right)\\ \vec{0}\end{pmatrix},\tag{16}$$

summarizes the evolution equations for the magnetohydrodynamic variables with conserved variables: $D=\gamma\rho$, $S_j=\rho h^*\gamma^2\upsilon_j-\alpha b^0b_j$, $E=\rho h^*\gamma^2-P$, $\upsilon^iB^j-B^i\upsilon^j$. Here, $h^*=1+\epsilon+P/\rho$ specific enthalpy from stress-energy tensor and $b^\mu=u_\nu F^{\mu\nu}$ from which $b^2=b^\mu b_\mu=2P$ magnetic pressure is obtained. Hence, compactly set by Jacobian determinant

$$\frac{\partial\boldsymbol{U}}{\partial t}+\boldsymbol{A}(U)\frac{\partial\boldsymbol{U}}{\partial x}=\boldsymbol{S}(U),\tag{17}$$

where $\boldsymbol{A}(U)$ is Jacobian matrix. For column matrix of flux we can have

$$J_F = \frac{\partial F_2}{\partial t} + \boldsymbol{A}(U)\frac{\partial F_2}{\partial x} = \boldsymbol{S}(y_2),$$

in the sense of linearized perturbations, that is lower terms of Equation (15), simplified over index $i = 1, 2, 3$ gives us

$$F_1 = \begin{pmatrix} Dv_1 \\ Dv_2 + P - B_1/\gamma \\ \rho v_1 v_2 - B_1 B - 2 \\ \rho v_1 v_3 - B_1 B_3 \\ 0 \\ \Omega_3 \\ -\Omega_2 \\ (E+P)\upsilon_1 - B_1(\boldsymbol{v}\cdot\boldsymbol{B}) - Dv_1 \\ \upsilon_1 B_2 - \upsilon_2 B_1 \end{pmatrix}, \tag{18}$$

imprecisely maintain the flow equation in cylindrical coordinate

$$\frac{\partial \rho v_r}{\partial t} + \frac{\partial}{\partial r}\left(\rho v_\phi^2 - B_\phi^2\right) + P/r = \frac{B_r B_\phi}{r},$$

including resistive term in the magnetized plasma. Therefore the conservative formulation Equation (14) has the general synthetic solution of the form

$$y(x) = y_0 \int f \mathrm{d}x, \tag{19}$$

where $f\mu(U) = \int \mu(U) S(U)$ and $\mu(U) = y_1^2 \exp\left(k(x)\mathrm{d}x\right)$. The integration can be solved analytically or numerically, where partial differential equation solver can be applied. Such numerically calculations are largely applied to MHD equations [30].

3. Disk Accretion Luminosity

The amount of energy dissipation and angular momentum transfer typical determine the accretion disk efficiency to convert gravitational energy into luminous radiation. The conservation of angular momentum prevents matter from falling directly into the hole in directions perpendicular to the rotation axis by centrifugal forces. The gas can, however, crumple along the rotation axis of the in falling torus so that a luminous disk of debris forms surrounding the hole, which is largely characterized by strong magnetic field, differential rotation and shear-induced turbulent stresses. The matter in this turbulent accretion disk can only fall into the rotating black hole if it loses angular momentum by turbulent stresses (strong magnetic or viscous forces) acting on the disk. Matter accreted from a geometrically thin disk reach the most stable inner circular orbit of radius r_I and continues freely falling into the chasm of black hole. Luminous radiation generated when debris of disk accreted into the black hole.

Using viscosity priscription $t_{r\phi} = \alpha\left(P_g + P_B\right) \approx \alpha \Sigma v_s^2$ [23] for gravitationally unstable rotating, relativistic thin and axisymmetric disk, the vertically averaged

surface density (Σ) is defined as the mass per unit surface area of the disk, given by integrating the gas density ρ in the *z*-direction

$$\Sigma(r,t)=\int_{-H}^{H}\rho(r,z,t)\mathrm{d}z=2\rho(r,t)H, \tag{20}$$

where, H is the scale height, when the gravitational force balanced with the vertical pressure gradient

$$H\approx\frac{\upsilon_s^2}{\Omega_K}\ll r, \tag{21}$$

is the disk half-thickness at radius *r*. Since $r\gg H$, the condition for height-integrated thin disk. We must have $\Omega_K\gg\upsilon_s$ and so the rotation of the disk is highly supersonic. Here for axisymmetric flows, cylindrical coordinates (r,ϕ,z) are employed with the z-axis chosen as the axis of rotation and the central plane of the disk lies in the equatorial plane of the kerr hole at $z=0$. It follows that the rate of mass flowing inward is readily integrated from mass conservation in equilibrium

$$\frac{1}{r}\frac{\partial}{\partial r}(r\Sigma\upsilon_r)+\frac{\partial}{\partial z}(\Sigma\upsilon_z)=0, \tag{22}$$

integrating to $r\Sigma\upsilon_r$ = constant. Here $\Sigma\upsilon_r$ is the inward flux of material and the mass accretion rate will be

$$\dot{M}=2\pi r\Sigma(-\upsilon_r), \tag{23}$$

a small inflow radial "drift" velocity υ_r is negative near the horizon, so that matter is being accreted. Since the fluid particles can experience magnetic resistive and viscous dissipation, the constraint equation is

$$\frac{\dot{M}}{4\pi}\frac{\mathrm{d}\ell}{\mathrm{d}r}+\frac{\mathrm{d}}{\mathrm{d}r}\left(r^2Ht_{r\phi}\right)+\frac{1}{r}\frac{1}{\mathrm{d}r}\left[r\left(v_rB_\phi-v_\phi B_r\right)\right]=0. \tag{24}$$

The whole accretion torus within accretion radius (outer edge of the disk) rotates about the hole with specific angular momentum of a circular disk

$$\ell\approx\Omega r_d^2=\sqrt{GM_Hr_d}=r\left(v_\phi-r^2\frac{B_r}{\dot{M}}B_\phi\right), \tag{25}$$

r_d is the radius where the outer edge of the disk forms.

Similarly, the angular momemtum conservation with viscous-stress tensor uniquely determines viscous accretion disk

$$\rho D_t\boldsymbol{V}=-\nabla\left(P+\frac{B^2}{2\mu_o}\right)+\frac{1}{\mu_o}(B\cdot\nabla)B+\rho\left(\frac{\chi}{c}\boldsymbol{F}-\Omega^2z\right)+\nabla\cdot\boldsymbol{t}, \tag{26}$$

where,

$$D_t=\frac{\mathrm{d}}{\mathrm{d}t}=\frac{\partial}{\partial t}+v_\beta\frac{\partial}{\partial x_\beta}=\frac{\partial}{\partial t}+v_r\frac{\partial}{\partial r}+v_z\frac{\partial}{\partial z}+v_\phi\frac{\partial}{\partial\phi}=\frac{\partial}{\partial t}+v\cdot\nabla.$$

The general form, including the viscous-stress tensor term (t_{ij}), simply expressed as

$$\rho D_tv_i=\rho g_i+\frac{\partial T_{ij}}{\partial j}+\rho\left(\frac{\chi}{c}\boldsymbol{F}-\Omega^2z\right)+\frac{1}{\mu_o}(B\cdot\nabla)B-\nabla\left(P+\frac{B^2}{2\mu_o}\right), \tag{27}$$

where $\boldsymbol{g}$ is force density and

$$T_{ij} = -P\delta_{ij} + t_{ij},$$

or we can typically express as

$$\rho D_t v_i = -\nabla P + \nabla \cdot \boldsymbol{t}, \tag{28}$$

where the viscous stress tensor (force density) $\boldsymbol{t}$ has components

$$t_{ij} = t_{ji} = \eta(\rho, T)\left[\nabla_i v_j + \nabla_j v_i - \frac{2}{3}\delta_{ij}\nabla \cdot v\right], \tag{29}$$

η is the dynamic or shear viscosity coefficient, usual known in kinetic molucler theory. Where we get the component $t_{r\phi}$ —a tangential viscous force per unit area exerted by the disk inside accretion radius:

$$t_{r\phi} = \eta r \frac{\mathrm{d}\Omega_k}{\mathrm{d}r} = \eta \nabla^2 v, \tag{30}$$

acts over an area ($2\pi rH$) of the disk for $\nabla \cdot v = 0$ from mass continuity equation. And Equation (28) will be

$$D_t v_i = -\frac{\nabla P}{\rho} + \frac{\eta}{\rho}\nabla^2 v, \tag{31}$$

where $\frac{\eta}{\rho} = \kappa_\nu = \alpha v_s H$ is kinematic viscosity. The disk tori in accretion radius rotates more rapidly and experiences a backward torque acting on the disk outside capture radius due to friction between adjacent layers of fluid elements generates a torque that carries angular momentum outwards.

$$\tau = (2\pi rH) r t_{r\phi} + r\left(v_\phi B_r - v_r B_\phi\right) = 2\pi\eta H r^3 \frac{\mathrm{d}\Omega_k}{\mathrm{d}r} + r\left(v_\phi B_r - v_r B_\phi\right), \tag{32}$$

is the torque generated by shear viscosity and magnetic forces, resulting in viscosity dominated turbulent magnetohydrodynamical stresses, where shear flows are stabilized by either differential rotation or strong magnetic fields. The gas spiral inwards and gradually loses angular momentum with transport rate $\dot{J} = \chi \dot{M} v_\phi - t_{r\phi} + \rho v_\phi^2 / \boldsymbol{X}$ through viscous force while the fluid outside capture radius gains the angular momentum. where χ is resistive (friction) coefficient in the fluid flows and $\dot{M} v_\phi$ is thrust: a force applied perpendicular to the area and $t_{r\phi} \sim \alpha\left(P_g + P_B\right) = \alpha \Sigma v_s^2$. Thus, the ϕ component of the momentum equation is

$$\rho\left(D_t v_\phi + \frac{v_r v_\phi}{r}\right) = \frac{1}{r}\partial_r\left(r t_{\phi r}\right) + \partial_z t_{\phi z} + \frac{1}{r} t_{r\phi}. \tag{33}$$

Here $t_{r\phi} = t_{\phi r}$ are the non-negligible components of t_{ij} in the disk's coordinates. Hence, using D_t in (33) gives

$$\partial_t\left(\rho r v_\phi\right) + \frac{1}{r}\partial_r\left(\rho r^2 v_\phi v_r\right) = \frac{1}{r}\partial_r\left(r^2 t_{r\phi}\right), \tag{34}$$

integrating over z gives

$$\partial_t \int \left(\rho r v_\phi\right) \mathrm{d}z + \int \frac{1}{r}\partial_r\left(\rho r^2 v_\phi v_r\right) \mathrm{d}z = \frac{1}{r}\partial_r\left(r^2 W_{r\phi}\right), \tag{35}$$

where $W_{r\phi}=\int t_{r\phi}\mathrm{d}z$ with increased pressure (stiff equation of state [31]). Using surface density, Equation (20), we can rewrite

$$\partial_t\left(\Sigma r v_\phi\right)+\frac{1}{r}\partial_r\left(\Sigma r^2 v_\phi v_r\right)=\frac{1}{r}\partial_r\left(r^2 W_{r\phi}\right). \tag{36}$$

The gradient of specific angular momemtum is the internal torques generated by shear viscosity and magnetic forces, resulting in viscosity dominated turbulent magnetohydrodynamical stresses. The radial component of angular momentum also determined as

$$\rho\left(D_t v_r-\frac{v_\phi^2}{r}\right)=-\rho r\Omega^2-\partial_r P+\frac{1}{r}\partial_r\left(r t_{rr}\right)+\partial_z t_{rz}-\frac{1}{r}t_{\phi\phi}. \tag{37}$$

The strongest viscous force exerted between two adjacent annulus of the disk is $t_{r\phi}$ component of the stress tensor, thus we shall assume that $t_{rr}=t_{\phi\phi}=0$. Equation (27) then simplifies to

$$\rho\left(\partial_t+v_r\partial_r\right)v_r=\rho\left(\frac{v_\phi^2}{r}-\Omega^2 r\right)-\partial_r P, \tag{38}$$

integrating

$$\Sigma\left(\partial_t+v_r\partial_r\right)v_r=\Sigma\left(\frac{v_\phi^2}{r}-\Omega^2 r\right)-\partial_r W, \tag{39}$$

where $W=\int P\mathrm{d}z$. Equation (39) states simply the radial hydrostatic pressure balance. Vertical gradients in the azimuthal field create vertical magnetic pressure gradients for an incompressible flow, are balanced by vertical fluid pressure gradients.

Using energy conservation equation we obtain the radiation energies emitted by accretion torus of rapidly spinning black hole. The basic equation for thin disk follows, from energy conservation Equation (13) is

$$\frac{\partial\varepsilon}{\partial t}+\nabla\cdot\left(\boldsymbol{S}+P\boldsymbol{v}+\rho\Phi_g\boldsymbol{v}\right)=\nabla\cdot\left(\boldsymbol{v}\cdot\boldsymbol{T}-\boldsymbol{h}\right)-\rho\frac{\mathrm{d}Q}{\mathrm{d}t}, \tag{40}$$

but consider various formulations of viscous stress tensor

$$T_{ij}=-P\delta_{ij}+t_{ij},$$

$$\nabla\cdot\left(\boldsymbol{v}\cdot\boldsymbol{T}\right)=\nabla\cdot\left(-P\delta_{ij}+t_{ij}\right)v_j=-PI+\boldsymbol{t},$$

gives pressure ($-\nabla\cdot\left(Pv\right)$) and viscous ($\nabla\cdot\left(\boldsymbol{v}\cdot\boldsymbol{T}\right)$) work. Heating due to viscous dissipation reduces kinetic energy.

$$\nabla\cdot\left(\boldsymbol{v}\cdot\boldsymbol{T}\right)=\frac{\partial\left(u_i T_{ij}\right)}{\partial x_j}.$$

Thus, the work on the disk due to forces on disk area is

$$\nabla\cdot\left(\boldsymbol{v}\cdot\boldsymbol{T}\right)=-\partial_j\left(Pv_j\right)+\partial_i\left(t_{ij}v_j\right), \tag{41}$$

substituting into (40) we get

$$\nabla\cdot\left(\boldsymbol{S}+P\boldsymbol{v}+\rho\Phi_g v\right)=-\nabla\cdot\boldsymbol{h}-\partial_j\left(Pv_j\right)+\partial_i\left(t_{ij}v_j\right), \tag{42}$$

for axisymmetric thin disk approximation $v_z = 0$, imply that

$$\partial_i \left(t_{ij} v_j \right) = \frac{1}{r} \partial_r \left(r t_{r\phi} v_\phi \right),$$

simple form for internal energy equation

$$\frac{\partial \left(\rho \varepsilon \right)}{\partial t} + \nabla \cdot \boldsymbol{K} = \nabla \cdot \left(\boldsymbol{v} \cdot \boldsymbol{T} \right) + \rho \frac{\partial Q}{\partial t} - \nabla \cdot \boldsymbol{h},$$

advection first term and the work done by $\nabla \cdot \boldsymbol{K}$ due to radiation $\nabla \cdot \boldsymbol{h}$, where radiation is due to viscous dissipation $\nabla \cdot \left(\boldsymbol{v} \cdot \boldsymbol{T} \right)$. Hence,

$$\nabla \cdot \left(\boldsymbol{S} + P\boldsymbol{v} + \rho \Phi_g v \right) = \frac{1}{r} \partial_r \left(r t_{r\phi} v_\phi \right) - \partial_r \left(P v_r \right) - \partial_z h_z.$$

Indeed, the steady-state mass conservation equation ensure

$$\nabla \cdot \vec{\boldsymbol{v}} \left(\rho \frac{v^2}{2} + \frac{P}{\Gamma - 1} + P + \rho \Phi_g \right) = 0,$$

where we are left with gradient of magnetic & turbulent viscosities result in gradient of energy flux density. Thus,

$$\frac{1}{r} \partial_r \left(r t_{r\phi} v_\phi \right) - \partial_r \left(P v_r \right) - \nabla \cdot \left(\frac{1}{\mu_0} B \times \left(v \times B \right) \right) = \partial_z h_z. \tag{43}$$

Equation (43) encompasses the differential rotation term ($t_{r\phi} v_\phi$), strong magnetic field ($B \times \left(v \times B \right)$), meridional circulation term ($grad \left(Pv - B \right)$) and shear induced turbulence term ($t_{r\phi}$) in the relativistic radiative MHD balanced with gradient of energy flux density (h_z). The heat diffuses toward the top and bottom surfaces of the disk where it is radiated away. Actually, the energy dissipated into heat due to viscousity is radiated in the vertical direction and radiation emitted along vertical midline from both surfaces of the disk (e.g. turbulent transport across sheared flows). Thus, we have vertical viscous dissipation per unit area (energy flux density $h_z = h_{vis} + h_B$) of disk surfaces given by

$$\partial_z h_z = \frac{\tau}{4\pi r} \partial_r \Omega, \tag{44}$$

with (30) and assuming Keplerian tangential velocity this becomes

$$\partial_z h_z = \frac{9}{8} \eta H \Omega_K^2 + \frac{\eta}{4\pi} \left| \nabla \times \boldsymbol{B} \right|^2,$$

with the help of (20) and (30), we generally determine vertical radiation energy flux density due to viscous dissipation as

$$h_z = \frac{9}{8} \kappa_\nu \Sigma \Omega_K^2 + \frac{\eta}{4\pi} \left| \nabla \times \boldsymbol{B} \right|^2, \tag{45}$$

is the rate of energy dissipation per unit volume due to the work done by the viscous forces. We know that torque is rate of change of angular momentum

$$\tau = \frac{\mathrm{d}J}{\mathrm{d}t} = \dot{M} \Omega r^2 = -2\pi r^2 H t_{r\phi}, \tag{46}$$

with (32) we will determine equality as

$$\dot{M}\left(\ell\left(r_d\right)-\ell\left(r_I\right)\right)=3\pi\eta H\left(GMr\right)^{1/2},$$

where, $\ell\left(r\right)=\Omega r^2=\left(GMr\right)^{1/2}$ and solving for η

$$\begin{aligned}\eta\left(r_I\right)&=\frac{\dot{M}}{3\pi H\left(GMr_d\right)^{1/2}}\left[\left(GMr_d\right)^{1/2}-\left(GMr_I\right)^{1/2}\right]\\&=\frac{\dot{M}}{3\pi H}\left[1-\left(\frac{r_I}{r_d}\right)^{1/2}\right],\end{aligned}\tag{47}$$

substituting into (45) we express radiation energy flux in terms of mass accretion rate as

$$h_z=\frac{3}{8\pi H}\dot{M}\Omega_K^2\left[1-\left(\frac{r_I}{r_d}\right)^{\frac{1}{2}}\right]=-\frac{\dot{M}v}{4\pi}\frac{\mathrm{d}\Omega_K}{\mathrm{d}r}\left(1-\frac{\ell_I}{\ell}\right),\tag{48}$$

is the rate of energy dissipation due to viscous forces. The maximum amount of heat is radiated away from the surfaces of the disk before matter accreted into the kerr hole. To determine the power of this radiation, consider a mass of luminous torus M_d falling from disk into the gravitational field of a rapidly rotating massive black hole with mass M_H. Therefore, integrating (48) over the two faces of the disk determine the total accretion power

$$L_{acc}=2\times 2\pi\int_{r_I}^{r_d}h_z r\mathrm{d}r,$$

establishes a maximal black hole disk accretion luminosity

$$L_{acc}=\frac{GM_{BH}\dot{M}_d}{2r_I}\propto\frac{\dot{M}_d}{r_I}=\dot{E}=\left(2\pi r^2\right)\left(2H\Omega\right)t_{r\phi},\tag{49}$$

the energy per unit time $\dot{E}$ dissipated in an annulus of width H.

The relativistic disk model parameters are: the black hole mass, M_H, and Kerr rotation parameter *a*, the mass accretion rate, $\dot{M}_d$, the inner r_I and outer r_d radii of the disk. **Figure 1** summarizes disk luminosity with range of mass accretion rate, $M_d=0.1M_\odot$, and initial $r_I=10^{10}\,\mathrm{m}$. Radiation luminosity drops as we go away from the black hole; for disk accretion rate of $\dot{M}_d=10^{-12}\,M_\odot/\mathrm{yr}$ [1], we obtain the accretion luminosity as less as 10^{28} erg/s at $r_I=10^{16}\,\mathrm{m}$, shown in **Figure 1**. But, for disk accretion rate of $M_d=10^{-9}\,M_\odot/\mathrm{yr}$, we obtain very high accretion luminosity comparable to Eddington luminosity (~10^{37} ergs/s) at $r_I=10^{10}\,\mathrm{m}$. An accretion rates $\dot{M}_d\sim 10^{-9}\,M_\odot/\mathrm{yr}\sim 10^{17}\,\mathrm{g/s}$ generate luminosity ~10^{37} ergs/s. When accretion rate increases, the luminosity linearly grows. The spectral flux was computed for a model with $M_H=10^7 M_\odot$, $\dot{M}=10^{19}\,\mathrm{g/s}$, $\theta=45^\circ$, $D=10\,\mathrm{kpc}$ and $r_I=10^4 r_g$ and obtained an accretion disk spectra with variations in black hole spin ($a=Jc/GM_H=0.35$, 0.7 and 0.998.), *i.e.*, rotation influenced flux as shown in **Figure 2**. These indicate that highly spinning black hole binaries emit shortest wavelength, energetic radiation (see **Figure 2**).

[1] $M_\odot/\mathrm{yr}=6.3\times 10^{25}\,\mathrm{g/s}$.

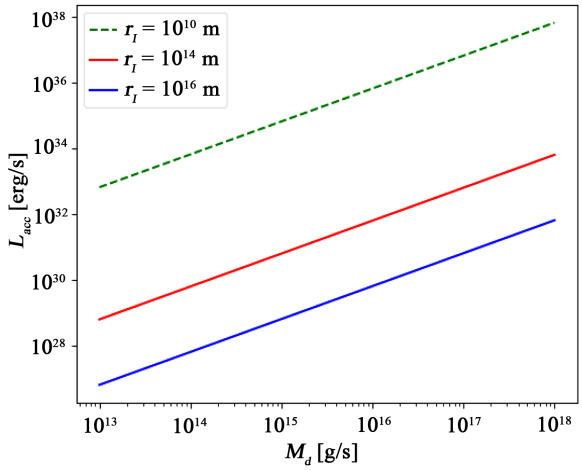

Figure 1. The accretion luminosity versus disk accretion rate at different values of innermost stable circular orbit radius (r_I).

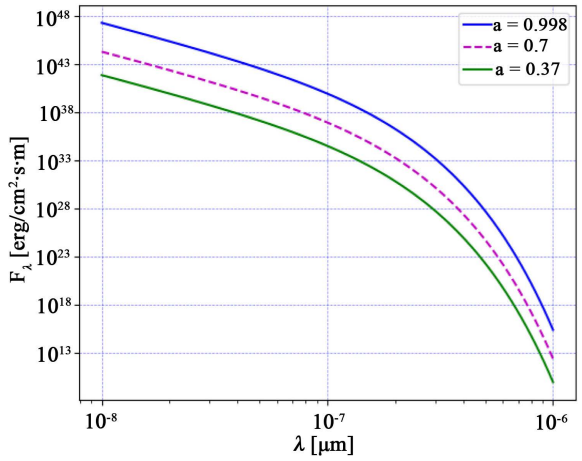

Figure 2. Flux density spectrum versus shortest wavelength emitted by a thin accretion disk around a rotating black hole at different values of Kerr rotation parameters a = 0.37, 0.7 and 0.998.

Thus, expressing the flux vector MHD Equation (14) in terms of the density terms, we formulate the general partial differential equations as

$$\frac{\mathrm{d}y}{\mathrm{d}x} + \chi f(x,y) = 0, \tag{50}$$

where y represents flux terms and x represents density terms such as mass, momentum and energy densities. Setting $f(x,y) = xy$ arbitrary function of source or sink, we obtain the radiation flux as

$$y = y_0 \exp\left(-\chi x^2\right), \tag{51}$$

where, $L_0 = 4\pi r^2 y_0 = GM\dot{M}/r$ and χ represents shear induced turbulant stresses with magneto-rotational instability enhance disk turbulence. In general, Poynting and radiation fluxes largely contribute to the luminosity

$$L = L_0 + S_{nuc} + S_{poyn} + S_{Ohm}, \tag{52}$$

with specific energy density ratio

$$\epsilon_B = \frac{4\phi\rho}{B^2}\left(v_r^2 + v_\phi^2\right). \tag{53}$$

The ratio ϵ_B is the magnetization function of magnetic flux.

4. Results and Discussion

We have studied the evolution of accreting BH in full general relativity including, imperfect MHD for viscous radiation. The relativistic accretion flow in resistive MHD and the resulting radiation basically explained as the X-ray luminosity of the central source, such as LMC X-1 and GRO J1655-40. LMC X-1 is a luminous X-ray source in the Large Magellanic Cloud (LMC). These results are interestingly consistent with observational data of galactic X-ray source binaries such as Cyg X-1, Cyg X-3 and Seyfert galaxies (NGC 3783, NGC 4151, NGC 4486 (Messier 87)). They are powerful emitters in X-ray and γ-ray wavebands. The spectrum of the observed hard X-ray flux exponential decays with energy is shown in Figure 3. The large luminosity of AGN (10^{46} erg/s) with the shortest wavelength can be explained by torus disk accretion process and accounts for observed X-ray rapid variability in the erratic light curves. The thin disk accretion onto extremely spinning magnetized BH is the likely source of high energy from binary X-ray sources. Typical X-ray source binary systems: Cyg X-1, LMC X-1, Cen X-3 (X-ray binary pulsar) and Cyg X-3 (X-ray luminosity of ~10^{31} J/s). The emission of X-ray flux is of synchrotron nature. For instance, the hard X-ray spectrum of the binary X-ray source Hercules X-1, as observed by the Ginga satellite displays synchrotron absorption at 35keV in high-intensity X-ray interaction with matter, shown in Figure 4.

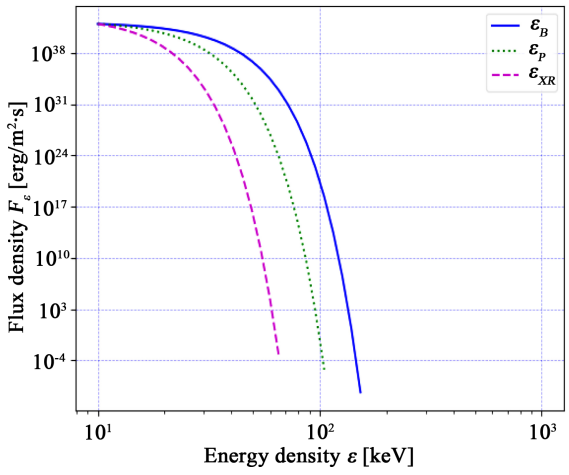

Figure 3. The luminosity flux spectrum of MHD disk radiation with magnetic, dynamical and gas pressure components. Steep decaying energy density (*i.e.* magnetic flux densities). Where $\epsilon_B = \frac{B^2}{25} = 1.5\times10^{-9}\,\mathrm{dyne/cm^2}$ magnetic flux densities, $\epsilon_P \sim \rho v^2 + P_{gas}$ dynamical energy density and ϵ_{XR} is the X-ray spectrum of X-ray binary Black Hole (Sco X-1). The X-ray differential energy spectrum in 10 - 10^3 KeV.

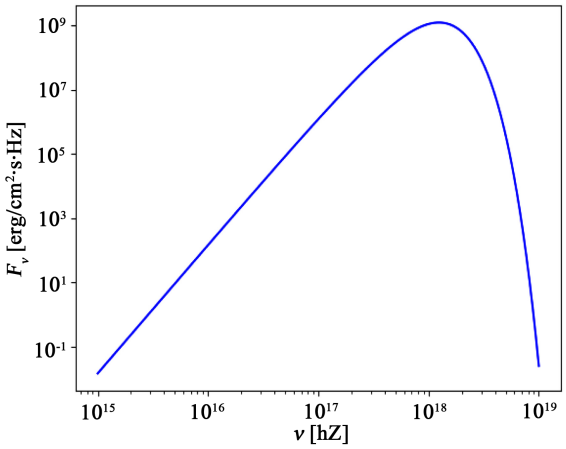

Figure 4. Frequency distribution of radiated energy flux density. The emission of X-ray and γ-ray fluxes are of synchrotron radiation type.

4.1. Thin Accretion Disk Radiation

Thin accretion disk luminosity $L_{acc} \sim 10^{30}\dot{M}_d/r_I$ as blackbody radiation with inner disk temperatures $T_d \sim \left(\dot{M}_d/r_I^3\right)^{\frac{1}{4}}$. A turbulent accreting disk emission spectrum consistent with the broad blackbody spectra (see 4) and also match to the synchrotron spectrum. For instance, the spectrum of Cyg X-1 [29] is the superposition of synchrotron radiation power law decay $E \propto t^{5/3}$ and blackbody spectrum with spectral luminosity $L_\nu \approx 10^{43}\,\mathrm{erg/s}\times\nu^{0.8}$ in the high frequency range. The luminosity spectrum of the disk can be approximated as a blackbody (**Figure 4**). The typical gas temperatures of 10^7 K at inner most radius made the flux is emitted from the inner face of the disk. At the inner disk boundary the local spectra contain an excess of high-energy photons in X-ray range (10^{17} Hz) display huge X-ray emission which can be fitted to observe X-ray data. As a result, the spectra obtained from a thin accretion disk around a Kerr black hole contains an energy maximum in the frequency range of the strong thermal X-ray sources. The radiation spectrum from an accretion disk around a Kerr black hole consistent with the observed spectrum of X-ray sources candidates. The spectral flux were computed for $M_B H = 10^7 M_\odot$, $\dot{M} = 10^{19}\,\mathrm{g/s}$, $\theta = 45^\circ$, $D = 10$ kpc and $r_I = 10^4 r_g$ and obtained an accretion disk spectra with variations in black hole spin ($a = Jc/GM_H = 0.35$, 0.7 and 0.998.), *i.e.*, rotation influence flux. For extremelly spinning ($a = Jc/GM_H = 1$) Kerr black hole, $r_I = r_g$. The black hole mass and spin, the accretion rate, the disk inclination angle and the inner disk radius are defining parameters of disk luminosity. The X-ray spectra of black hole binaries observed so far, LMC X-1, GRO J1655-40, PSO J334+01 spectrum significantly infer disk accreting Kerr hole. The model then anticipates that geometrically thin, optically thick disks in black hole binaries radiate X-rays (3×10^{16} Hz). The structure of the radio lobes observed in super-critical PSO J334+01 spectrum significantly infer massive BH coalescence. At high frequencies, scattering opacity effects are useful and result in a modified Wien spectrum. For

high accretion rate ($\dot{M}$) and viscous alpha spectrum peak appears in the soft X-ray range, where disk becomes optically thin. The high-energy photons at r_I and the disk rotation shifts up to the photon frequencies determine all flux frequency band of a thin accretion disk (see Figure 4) and at high γ-ray energy the spectrum is steepy exponential decay form. For example, the X-ray continuum of binary X-ray pulsars is characterized by a power-law of photon index of α = 0.3 - 2 with an exponential cuttoff at high energies (MeV), because light-curve features (plateau and the flare) are constrainted by high energy emission. Therefore, a significant amount of the total flux is emitted in the soft X-ray range. Most of the flux is emitted in the UV band ($\nu \geq 2\times 10^{15}\,\mathrm{Hz}$) up to the X-ray range ($\nu \geq 10^{17}\,\mathrm{Hz}$) at typical gas temperature of $T_I = 10^5\,\mathrm{K}$ from $M_H = 10^8 M_\odot$. These estimates are sufficient for modeling the majority of accretion disk spectra from observed black hole X-ray bursts. A black hole with mass $M_H = 10^8 M_\odot$ emits X-ray luminosities of 10^{47} erg/s identified.

4.2. Conclusion

We have summarized that high-energy GRBs generated by rotating black hole-accretion disk system. Basic analyses of Figure 1 deduce that accretion luminosity drops as we go away from the central Kerr black hole. This probes the energy injection that generates plateau phase as well as x-ray flares. The radiation flux as function of emitted photon frequency and energy density explained the engine as accreting compact binary galactic X-ray emitters. The observed luminosity in X-ray ranges for active galactic nuclei tell us, hard X-ray emission from galactic compact binary systems, typical X-ray source binaries, scorpius X-1 [32]. Early X-ray light curve components with large luminosities imply accretion disk radiation of these progenitors where, the total flux is emitted in the soft X-ray energy range shown in Figure 3. Thin disk radiates locally as a blackbody above critical frequency as shown in Figure 3, indicate that the total flux is emitted in the soft X-ray range at high frequency due to Poynting, magnetic and radiation pressure fluxes as studied in Equation (51) and the result shown in Figure 3. The spectral evolution resembles that of high energy particle acceleration. Particularly, synchrotron and multi-colour blackbody contribution (see Figure 4). The electron energy distribution in the most stable inner radius (r_I) gets hotter due to transition of bulk kinetic energy into thermal energy, following a power-law distribution. The synchrotron spectrum slopes as ν^2 at low frequencies and scales as ($\nu^{(1-p)/2}$), where $p \approx 2.4$ is the power-law index for the energy distribution of electrons. High Lorentz factor γ_c electrons cool more rapidly, and this causes a break in the synchrotron spectrum at a critical cooling frequency ν_c.

Acknowledgements

I thank Addis Ababa University, Jijiga University and Adama Science and Technlogy University for all support made.

Conflicts of Interest

The authors declare no conflicts of interest regarding the publication of this paper.

References

[1] Metzger, B.D. and Bower, G.C. (2014) Constraints on Long-Lived Remnants of Neutron Star Binary Mergers from Late-Time Radio Observations of Short Duration Gamma-Ray Bursts. *Monthly Notices of the Royal Astronomical Society*, **437**, 1821-1827. https://doi.org/10.1093/mnras/stt2010

[2] D'Avanzo, P. (2015) Short Gamma-Ray Bursts: A Review. *Journal of High Energy Astrophysics*, **7**, 73-80. https://doi.org/10.1016/j.jheap.2015.07.002

[3] Lyons, N., O'Brien, P.T., Zhang, B., Willingale, R., TRoja, E. and Starling, R. (2010) Can X-Ray Emission Powered by a Spinning-Down Magnetar Explain Some Gamma-Ray Burst Light-Curve Features? *Monthly Notices of the Royal Astronomical Society*, **402**, 705-712. https://doi.org/10.1111/j.1365-2966.2009.15538.x

[4] Woosley, S.E. and Heger, A. (2006) The Progenitor Stars of Gamma Ray Bursts. *The Astrophysical Journal*, **637**, 914-921. https://doi.org/10.1086/498500

[5] Font, J.A., Rezzolla, L., Giacomazzo, B., Baiotti, L. and Link, D. (2011) Towards Modelling the Central Engine of Short GRBs. *Journal of Physics: Conference Series*, **314**, Article ID: 012013. https://doi.org/10.1088/1742-6596/314/1/012013

[6] Woosley, S.E. (1993) Gamma-Ray Bursts from Stellar Mass Accretion Disk around Black Holes. *The Astrophysical Journal*, **405**, 273-277. https://doi.org/10.1086/172359

[7] Bucciantini, N., Quataert, E., Metzger, B.D., Thompson, T.A., Arons, J. and Del Zanna, L. (2009) Magnetized Relativistic Jets and Long-Duration GRBs from Magnetar Spin-Down during Core-Collapse Supernovae. *Monthly Notices of the Royal Astronomical Society*, **396**, 2038-2050. https://doi.org/10.1111/j.1365-2966.2009.14940.x

[8] Cerda-Duran, P. and Elias-Rosa, N. (2018) Neutron Stars Formation and Core Collapse Supernovae. In: Rezzolla, L., Pizzochero, P., Jones, D.I. and Vidaña, N.R., Eds., *The Physics and Astrophysics of Neutron Stars*, Springer, Berlin, 1-56. https://arxiv.org/pdf/1901.09977.pdf https://doi.org/10.1007/978-3-319-97616-7_1

[9] Shibata, M. and Kiuchi, K. (2017) Gravitational Waves from Remnant Massive Neutron Stars of Binary Neutron Star Merger: Viscous Hydrodynamics Effects. *Physical Review D*, **95**, Article ID: 123003. https://doi.org/10.1103/PhysRevD.95.123003

[10] Giacomazzo, B., Zrake, J., Duffell, P.C., MacFadyen, A.I. and Perna, R. (2015) Producing Magnetar Magnetic Fields in the Merger of Binary Neutron Stars. *The Astrophysical Journal*, **809**, 39. https://doi.org/10.1088/0004-637X/809/1/39

[11] Proga, D., MacFadyen, A.I., Armitage, P.J. and Begelman, M.C. (2003) Axisymmetric Magnetohydrodynamic Simulations of the Collapsar Model for Gamma-Ray Bursts. *The Astrophysical Journal*, **599**, L5. https://doi.org/10.1086/381158

[12] Margutti, R., Bernardini, G., Barniol Duran, R., Guidorzi, C., Shen, R.F. and Chincarini, G. (2011) On the Average Gamma-Ray Burst X-Ray Flaring Activity. *Monthly Notices of the Royal Astronomical Society*, **410**, 1064-1075. https://doi.org/10.1111/j.1365-2966.2010.17504.x

[13] Narayan, R., Sadowski, A. and Soria, R. (2017) Spectra of Black Hole Accretion Models of Ultra Luminous X-Ray Sources. *Monthly Notices of the Royal Astronomical Society*, **469**, 2997-3014. https://doi.org/10.1093/mnras/stx1027

[14] Siegel, D.M. and Metzger, B.D. (2018) Three-Dimensional GRMHD Simulations of Neutrino-Cooled Accretion Disks from Neutron Star Mergers. *The Astrophysical Journal*, **858**, 52. https://doi.org/10.3847/1538-4357/aabaec

[15] Rezzolla, L., Most, E.R. and Weih, L.R. (2018) Using Gravitational-Wave Observations and Quasi-Universal Relations to Constrain the Maximum Mass of Neutron Stars. *The Astrophysical Journal Letters*, **852**, L25. https://doi.org/10.3847/2041-8213/aaa401

[16] Kumar, P., Narayan, R. and Johnson, J.L. (2008) Mass Fall-Back and Accretion in the Central Engine of Gamma-Ray Bursts. *Monthly Notices of the Royal Astronomical Society*, **388**, 1729-1742. https://doi.org/10.1111/j.1365-2966.2008.13493.x

[17] Proga, D. and Zhang, B. (2006) The Late Time Evolution of Gamma-Ray Bursts: Ending Hyperaccretion and Producing Flares. *Monthly Notices of the Royal Astronomical Society*, **370**, L61-L65. https://doi.org/10.1111/j.1745-3933.2006.00189.x

[18] Baiotti, L. and Rezzolla, L. (2017) Binary Neutron Star Mergers: A Review of Einstein's Richest Laboratory. *Reports on Progress in Physics*, **80**, Article ID: 096901. https://doi.org/10.1088/1361-6633/aa67bb

[19] Abbott, B.P., Abbott, R., Abbott, T.D., Acernese, F., Ackley, K., Adams, C., Adams, T. and Addesso, P. (2017) GW170817: Observation of Gravitational Waves from a Binary Neutron Star Inspiral. *Physical Review D*, **119**, Article ID: 161101. https://doi.org/10.1103/PhysRevLett.119.161101

[20] Paschalidis, V. (2017) General Relativistic Simulations of Compact Binary Mergers as Engines for Short Gamma-Ray Bursts. C*lassical and Quantum Gravity*, **34**, Article ID: 084002. https://doi.org/10.1088/1361-6382/aa61ce

[21] Porth, O., Olivares, H., Mizuno, Y., Younsi, Z., Rezzolla, L., Moscibrodzka, M., Falcke, H. and Kramer, M. (2017) The Black Hole Accretion Code. https://arxiv.org/pdf/1611.09720.pdf https://doi.org/10.1186/s40668-017-0020-2

[22] Fryer, C.L., Belczynski, K., Ramirez-Ruiz, E., Rosswog, S., Shen, G. and Steiner, A.W. (2015) The Fate of the Compact Remnant in Neutron Star Mergers. *The Astrophysical Journal*, **812**, 24. https://doi.org/10.1088/0004-637X/812/1/24

[23] Shakura, N. and Sunyaev, R. (1976) A Theory of the Instability of Disk Accretion on to Black Holes and the Variability of Binary X-Ray Sources, Galactic Nuclei and Quasars. *Monthly Notices of the Royal Astronomical Society*, **175**, 613-632. https://doi.org/10.1093/mnras/175.3.613

[24] Zdziarski, Andrzej, A., Malzac, J. and Bednarek, W. (2009) A Model of the TeV Flare of Cygnus X-1: Electron Acceleration and Extended Pair Cascades. *Monthly Notices of the Royal Astronomical Society*, **394**, 41. https://doi.org/10.1111/j.1745-3933.2008.00605.x

[25] Komissarov, S.S. and Barkov, M.V. (2007) Magnetar-Energized Supernova Explosions and Gamma-Ray Burst Jets. *Monthly Notices of the Royal Astronomical Society*, **382**, 1029-1040. https://doi.org/10.1111/j.1365-2966.2007.12485.x

[26] Chincarini, G., Moretti, A., Romano, P., Falcone, A.D., Morris, D., Racusin, J., Campana, S., Covino, S., Guidorzi, C., Tagliaferri, G., Burrows, D.N., Pagani, C., Stroh, M., Grupe, D., Capalbi, M., Cusumano, G., Gehrels, N., Giommi, P., La Parola, V., Mangano, V., Mineo, T., Nousek, J.A., O'Brien, P.T., Page, K.L., Perri, M., Troja, E., Willingale, R. and Zhang, B. (2007) The First Survey of X-Ray Flares from

Gamma-Ray Bursts Observed by Swift: Temporal Properties and Morphology. *The Astrophysical Journal*, **671**, 1903-1920. https://doi.org/10.1086/521591

[27] Sadowski, A. (2016a) Magnetic Flux Stabilizing Thin Accretion Disks. *Monthly Notices of the Royal Astronomical Society*, **462**, 960-965. https://doi.org/10.1093/mnras/stw1852

[28] Fan, Y.-Z., Yu, Y.-W., *et al*. (2013) A Supra-Massive Magnetar Central Engine for GRB 130603b. *The Astrophysical Journal*, **779**, L25. https://doi.org/10.1088/2041-8205/779/2/L25

[29] Mandal, S. and Mondal, S. (2018) Spectral Properties of the Accretion Disks around Rotating Black Holes. *Journal of Astrophysics and Astronomy*, **39**, 19. https://doi.org/10.1007/s12036-017-9509-y

[30] McKinney, J.C., Chluba, J., Wielgus, M., Narayan, R. and Sadowski, A. (2017) Double Compton and Cyclo-Synchrotron in Super-Eddington Disks, Magnetized Coronae and Jets. *Monthly Notices of the Royal Astronomical Society*, **467**, 2241-2265. https://doi.org/10.1093/mnras/stx227

[31] Radice, D., Perego, A., Zappa, F. and Bernuzzi, S. (2018) GW170817: Joint Constraint on the Neutron Star Equation of State from Multi Messenger Observations. *The Astrophysical Journal Letters*, **852**, L29. https://doi.org/10.3847/2041-8213/aaa402

[32] Revnivtsev, M.G., Tsygankov, S.S., Churazov, E.M. and Krivonos, R.A. (2014) Hard X-Ray Emission of Sco X-1. *Monthly Notices of the Royal Astronomical Society*, **445**, 1205-1212. https://doi.org/10.1093/mnras/stu1831